Experimental Investigation of the Flexural Performance of Hybrid Carbon and Steel Reinforced Concrete Beams

Amr Sobhey Abdelrahim Radi
Ph.D. Student,Faculty of Engineering Helwan University, Ibrahim Abdel-Razek St. Ain Shams, Cairo.
Email: amrsobhy936@gmail.com
Mohammed M. Soliman
Teacher of R.C. Structures, Faculty of Engineering BenhaUniversity, shobra , Cairo.
Magdy M.M. Genidi
Assistant Professor of R.C. Structures, Faculty of Engineering Helwan University, Ibrahim Abdel-Razek St. Ain Shams, Cairo
Email: magdy_genidi@yahoo.com

Abstract:

Corrosion of steel reinforcing bars is a major factor in concrete structures' failure to endure prolonged exposure to weather. In concrete constructions, fiber-reinforced polymer (FRP) reinforcement has replaced steel reinforcement as a viable solution to this issue. One disadvantage of CFRP is its brittleness and expensive cost. The main goal of this project is to design a viable hybrid FRP bar for concrete structures, notably marine and port concrete construction. Because CFRP bars with adequate tensile strength may be improved by hybridization, the elastic modulus and flexibility of CFRP bars can be increased, and corrosion protection can be improved. The development of CFRP crust with steel core bar and CFRP crust with steel core bar is being evaluated as forms of hybrid FRP bar. Because of hybridization with other materials, this study found an increase in the elastic modulus and stiffness of the hybrid GFRP bar. Produced utilizing local raw materials and a two-part die mold, the bars are locally sourced. For the flexural limit states of sixteen beams with dimensions of 200 mm in width by 350 mm in thickness by 2000 mm in length, researchers used four-line static loading to investigate pre-cracking behavior, cracking pattern, deflection, load capacity, and strain.

Keywords: Concrete, beams, Failure, FRP Composites, Hybrid FRP, locally produced.

1. INTRODUCTION

There are numerous production processes for FRP composites; these technologies, such as pultrusion, wet lay-up, and injection molding, are detailed in the ACI 440 reports (1996–2015). used in the design and manufacturing of FRP bars for use in reinforced concrete members. It is possible to produce long, straight, constant cross-section components constructed of reinforced polymeric composites using only one continuous, completely automated manufacturing process (the pultrusion process).

Reinforcing materials in the form of continuous rods, mats, and other types of fabric are drawn through a resin matrix bath or other impregnation device and then carefully passed through a preform station followed by a heated high-precision die where the resin matrix cures at a high temperature to form the final product in pultrusion. In the end, a saw is used to cut the cured profile into predefined lengths after it has been continually drawn through the saw.

In this study, the hybridization effect is investigated as a function of the amount of hybrid material, considering glass fiber, carbon fiber, and steel (i.e., as hybrid materials). The hybrid bars are produced on site in a two-part mold using local raw materials.

Several investigations into concrete slabs and beams reinforced with HFRP bars have been conducted in recent years.

In addition, high-performance concrete is being developed for the construction of large and important structures and high-rise buildings. High-strength concrete (HSC) is a type of high-performance concrete developed to improve strength. High strength concrete provides higher compressive strength, higher modulus of elasticity, higher tensile strength, lower creep and greater durability than normal strength concrete. For the same cross-section and span, a beam made of high-strength concrete has a lower initial deflection, a higher allowable tensile stress, and a longer service life than a similar beam made of normal-strength concrete.

Thus, this paper is devoted to defining the problem that challenges engineers and that the researcher wants to address. The chapter also gives an overview of hybrid fiber reinforced polymer (HFRP) bars and high strength concrete and their classification. The objectives of the study are also explained in this chapter. Finally, the structure of the thesis is outlined.

2. EXPERIMENTAL WORK

This paper presents the major experimental program devised to explore the behavior of HFRP-reinforced concrete simple-span beams. Five simply supported concrete beams reinforced with HFRP and two simply supported concrete beams reinforced with CFRP. For comparative reasons, two steel-reinforced concrete beams are also being evaluated as a control group. It is important to note that in this investigation, a variety of HFRP reinforcing bar combinations and types, as well as concrete strength, were tested.

This paper is also devoted to an account of the experimental work. It gives the details of the specimens. It also describes the properties of the materials used. It describes the preparation of the specimens and the investigation of their mechanical properties. Finally, the load structure of the investigated specimens is presented.

2.1. Chartings the Specimens Details

The type of HFRP-reinforced bars, the strength of concrete, and the type of fiber are the main parameters studied, which are summarized in Table 1 and Figure 1. The concrete beams reinforced with HFRP are reinforced with three different types of hybrid reinforcing bars.

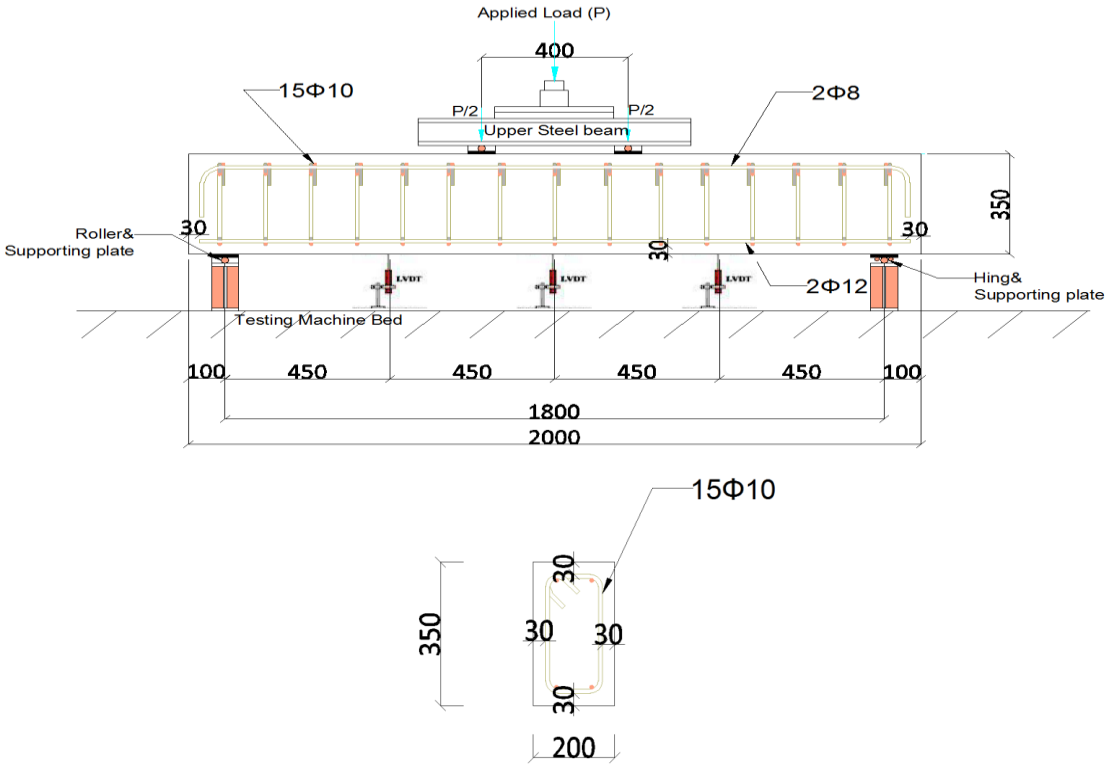

Figure 1. Experimental details of HFRP beams.

Table 1: Designation of beams and characteristics of longitudinal reinforcement and concrete

Beam Notation	Tensionreinforcement bottom reinforcement Rebar type &Quantity		Steel-to- GFRP ratio %	Concrete properties		Remark
	No.	Type		F_{cu} MPa	F_{ct} MPa	
A-1-S (CONTROL)		STEEL	100%	30	3.28	H-T STEEL
A-3-C (CONTROL)		CFRP	0%	30	3.28	CFRP
A-6-H		HFRP(D)	44%	30	3.28	HFRP Ø 8-C
A-7-H		HFRP(F)	69%	30	3.28	HFRP Ø 10-C
A-9-H		HFRP(B)	25%	30	3.28	HFRP Ø 6-G
B-1-S (CONTROL)		STEEL	100%	62.5	4.91	H-T STEEL
B-3-C (CONTROL)		CFRP	0%	62.5	4.91	CFRP
B-6-S		HFRP(E)	44%	62.5	4.91	HFRP Ø 8-C
B-7-S		HFRP(F)	69%	62.5	4.91	HFRP Ø 10-G

C*carbon fiber HFRB*hybrid bar

Figure 2 shows types of bars that have ribbed surfaces. To analyze the influence of steel hybridization on tensile performance, the different steel volume fractions to cross-sectional area and the kind of FRP are parameterized in table 2.

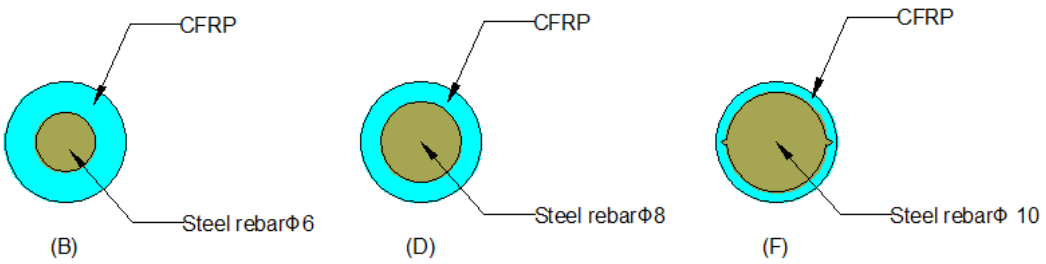

Figure 2. Cross section types of "FRP Hybrid Bar" [HFRP].

(b) CFRP crust with a steel rod (six millimeters) in the core (d) CFRP crust with a steel rod (eight millimeters) in the core;(f) CFRP crust with a steel rod (ten millimeters) The height of the ribs is not included in the HFRP's diameter.

Table 2: Details of the manufactured hybrid bars

Group Code	Fiber Type Used	SpecimenCode	No. of Filament Glass	Steel Rebar Diameter (ϕ) mm	Steel / GFRP ratio %
CF Rebars	GlassFiber	CF	66	–	0%
HFRP Rebars	Carbon/ Steel rebar	HFRP-B	30	6	25%
		HFRP-E	20	8	44%
		HFRP-F	10	10	69%

Figure 3. : Final product for development of FRP Hybrid Bars.

2.2.Tensile Strength Test

The test equipment and the UH with a capacity of 1000 kN and a maximum stroke length of 500 mm are shown in Figures 4. Both the top and bottom of the specimens are clamped to

the steel clamping adapters. A data logger is used to record the load and the accompanying stresses.

Figure 4. : Tensile test setup.

The results of all bar tension tests may be seen in the table below. These tests were performed on the UH–1000kn–machine on eight specimens. In order to meet the minimum tensile specimen requirements recommended by ACI-440, the specimens are provided with a special setup consisting of a steel tube to attach the specimen anchor to the load cell. Brittle fracture was one of FRP's shortcomings, which was confirmed to be alleviated by the material hybridization (i.e., "pseudo ductile" behavior) shown in Figure 5 (a, b, c).

3. TEST RESULTS AND DISCUSSION

3.1.Tensile Strength Test

Figure 5. Overall View of Failed HFRP Specimen core

(a) Normal FRP failure

(b) HFRP with steel rebar in core at failure in CFRP and necking fracture.

(c) HFRP bar with steel rebar in core at failure

Figure 6. Failure of normal CFRP and HFRP bar specimens.

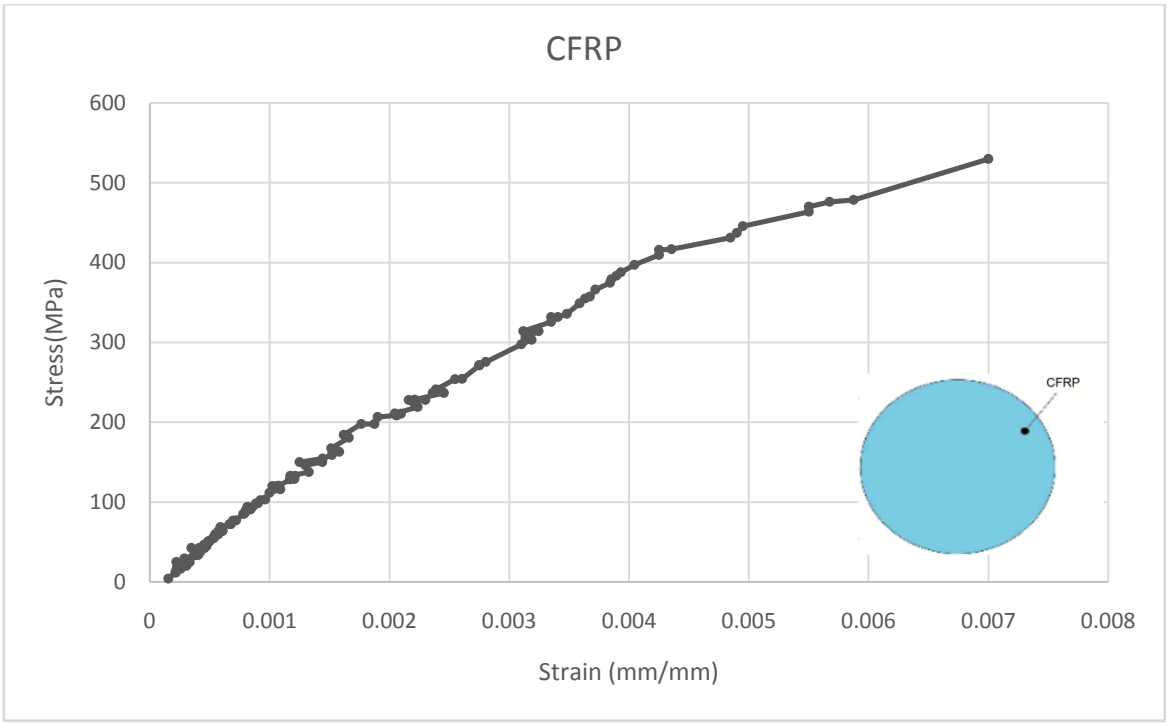

Figure 7. Stress-strain relationship for pure CFRP bar.

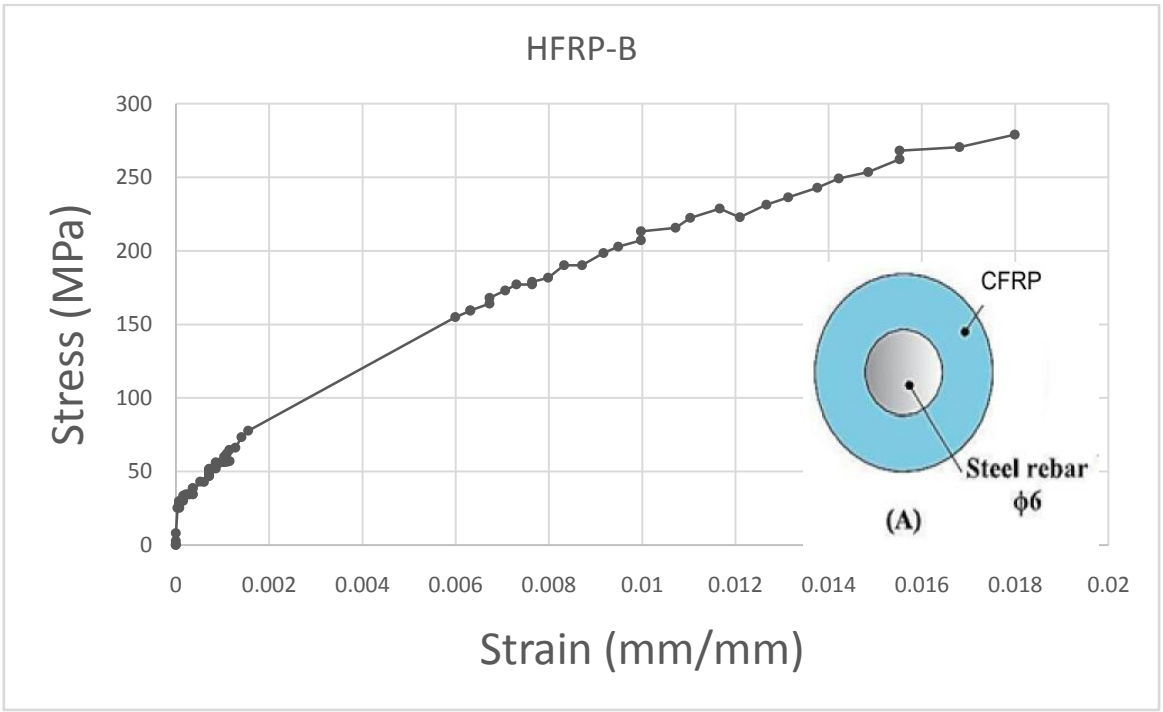

Figure 8. Stress-strain relationship for Hybrid bar Type B.

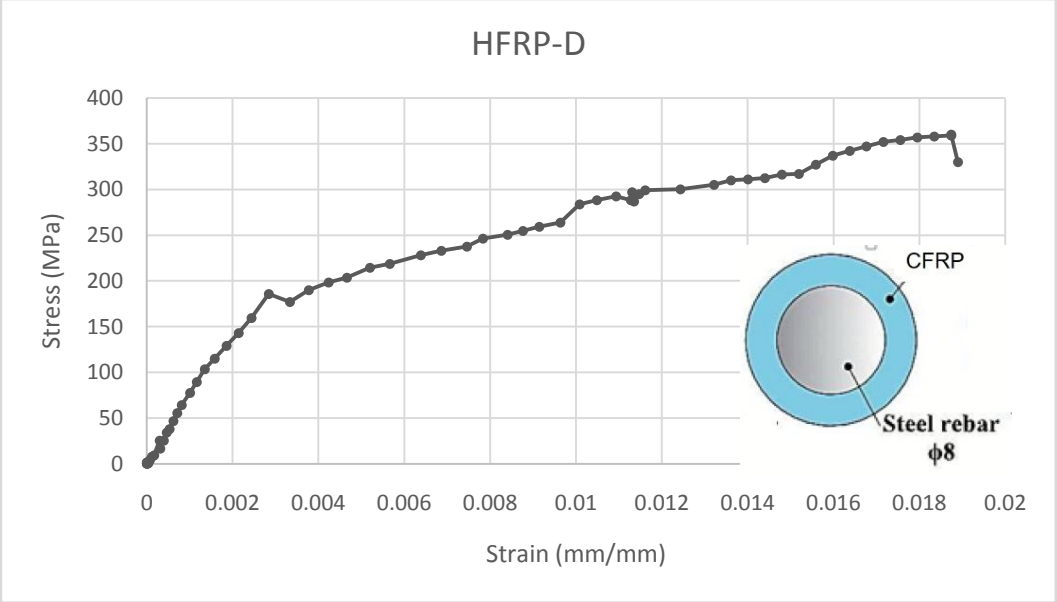

Figure 9. Stress-strain relationship for Hybrid bar Type D.

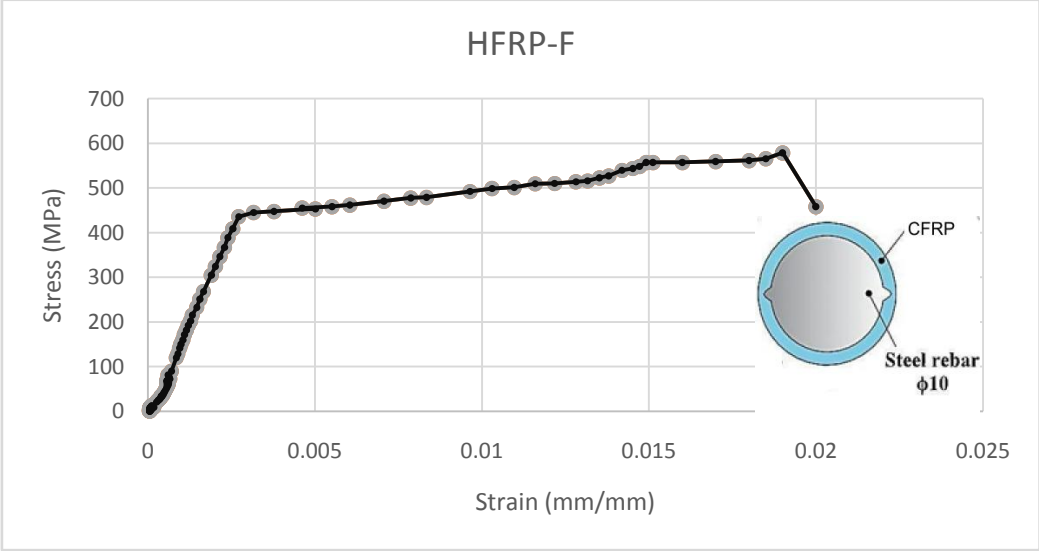

Figure 10. Stress-strain relationship for Hybrid bar Type F.

Table 3: Test results for Steel,CFRB and Hybrid Bar

Type of bar	Average ultimate Load,	Elastic Modulus		Tensile Strength	Ultimate Strain	
	Pu (KN)	Aver. (GPa)	Imp. (%)	(MPa)	%	Imp. (%)
STEEL	73.5	200	387.80	650.44	0.032	50.94&357
CFR(Ref.)	61	42	--	531	0.007	0.00
HFRP-B	31.5	48	14.2	278.93	0.013	85.7
HFRP-D	40.67	73	73.80	359.92	0.0189	170
HFRP-F	66.43	173.3	312.61	587.90	0.02	185

The Test Method for Tensile Properties of FRP Reinforcement can be used to calculate the elastic modulus of an FRP Hybrid Bar (Ehybrid).

$$E_h = \frac{(P_1 - P_2}{(\varepsilon_1 - \varepsilon_2)A_h}$$

Where $P1$ and $\varepsilon 1$ are the load and corresponding strain respectively, at approximately 50% of the ultimate tensile capacity, while $P2$ and $\varepsilon 2$, are the load or the corresponding strain at about 25% of the ultimate tensile strength.

In Figures 8 through 10, the ultimate tensile strength for (Types D, E, and F) has 278.93MPa, 359.93MPa, and 587.90MPa, respectively. This phenomenon is due to the fact that the steel bar with lower tensile strength dominated and failed before the CFRP. It is found that the increased ranges of modulus of elasticity showed from 14.2 to 312.61 % as compared because the tensile stress-strain behaviors of steel core are identical table 3.

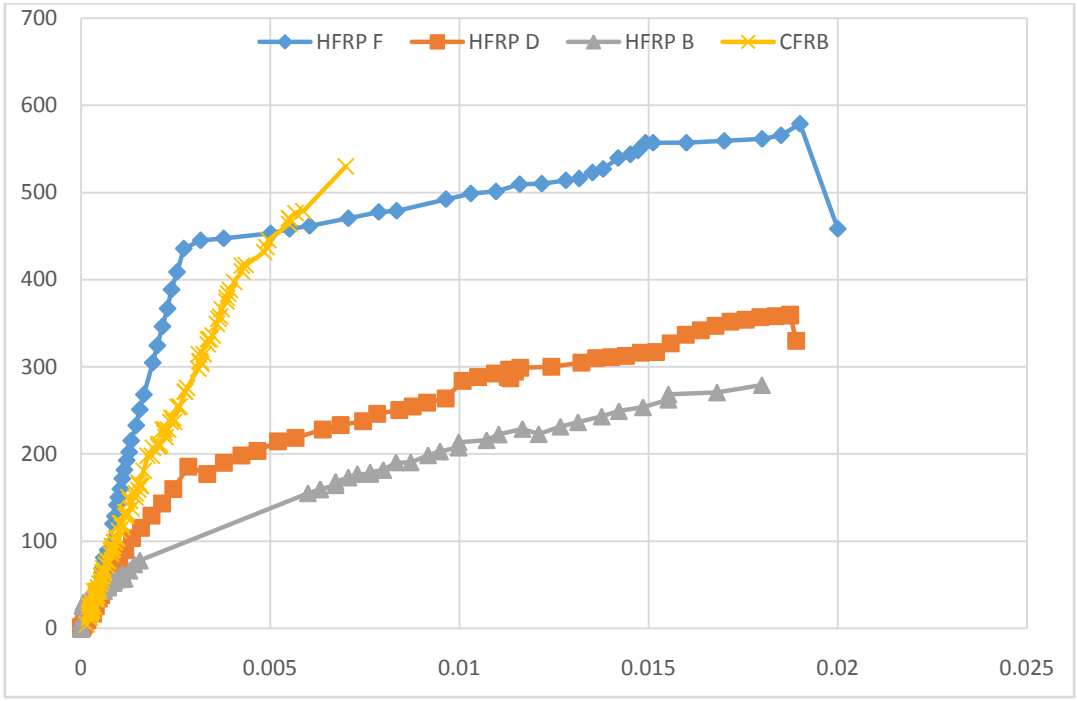

Figure 11. Comparison between GFRP and HFRP (B, D and F) bars.

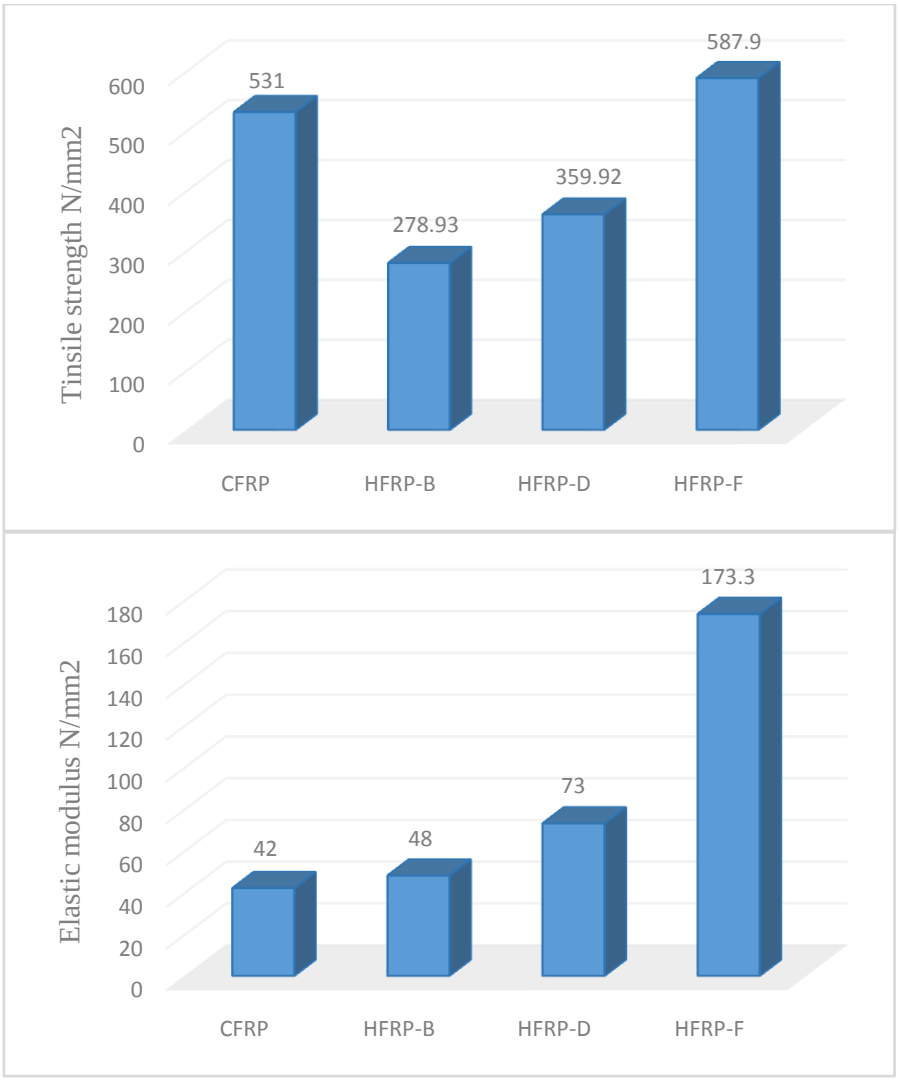

Figure 12. Comparison of the test results for HFRP (B, D and F) with CFRP: (a) elastic modulus; (b) tensile strength.

Figure 13.

3.2.Flexural Behavior of beams under static Four Point Line Loading

Mode 1: Rupture of CFRP Failure. This mode is experienced by beams 2C12 reinforced with under reinforcement of CFRP. It was found that the first visible flexural cracks occurred in beams A-3-C at a load of 31.2 kN. For the high-strength concrete B-3-C, the first visible flexural cracks occurred at a load of 50 kN. Predictably, the strain in the CFRP reinforcement reaches its ultimate capacity at mid-span before the ultimate capacity of the concrete fails completely, which normally leads to this failure mode. It should be noted that the failure of CFRP bars occurs suddenly and is accompanied by a loud noise, which means a rapid release of energy. Therefore, we can overcome this problem by using the newly developed hybrid rod presented in this paper. A-3-C failed at a load of 80 kN,. B-3-C failed at a load of 90Kn.

Figure 14. Flexure failure at mid span of beam A-3-C.

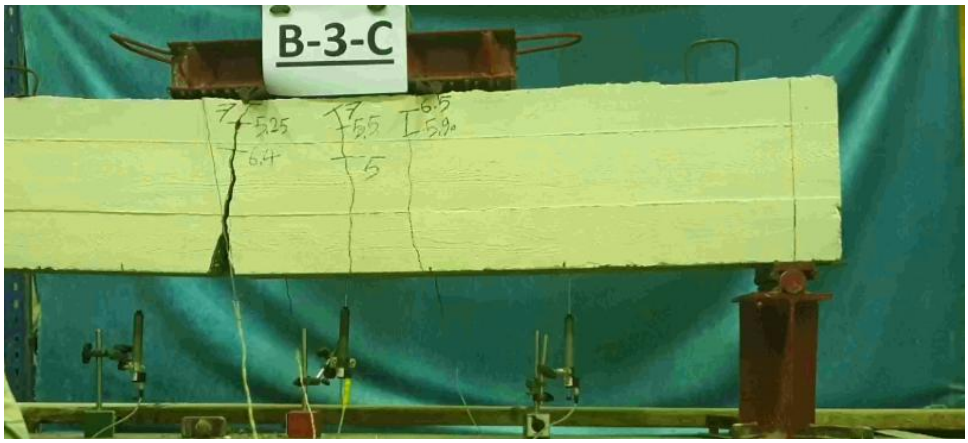

Figure 15. Flexure failure at mid span of beam B-3-C.

Mode 2: For all remaining beams, conventional ductile flexural failure occurred owing to yielding of tensile steel or hybrid FRP reinforcing bar followed by concrete crushing at mid-span. Because steel bars had a greater axial stiffness than HFRP bars, the steel reinforced concrete beam had a larger initial cracking load than the HFRP reinforced concrete beam. The initial cracking load was also impacted by the ratio of hybridization of each kind of HFRP reinforcing bar in the various beams tested. Tension failure, i.e., rebar giving and eventually concrete crushing failure, is visible in all beams.

The crack pattern at failure of the beam B-1-S with reinforcing steel bars and high-strength concrete is depicted in Figures 15 and 16.It should be noted that both beams are tested under increasing static loads up to failure. It is observed that the first visual flexural crack for beam A-1-S appeared at the bottom of the beam at the mid-span location at loads of 40 Kn and 49.2 for B-1-S. Cracks developed in the region of maximum moment below or between point loads and propagated upward toward the compressed concrete zone. As the load increased, more cracks occurred along the beam, and the cracks in the shear spans inclined towards the central zone. Failure occurs when one or more cracks in the zone of maximum moment extend to the upper concrete fibers in the maximum moment zone, leading to concrete crushing. A-1-S failed at a load of 134 kN and B-1-S failed at a load of 152 kN.

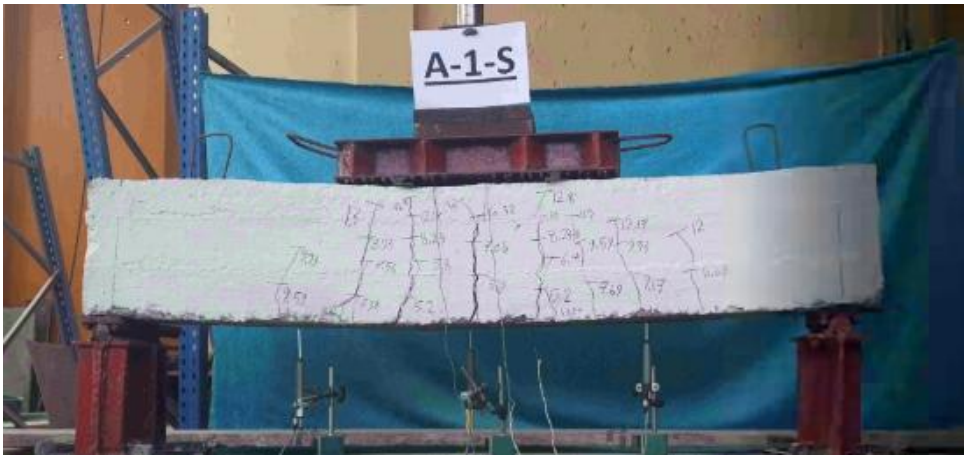

Figure 16. Conventional ductile flexural failure mode of steel A-1-S.

Figure 17.

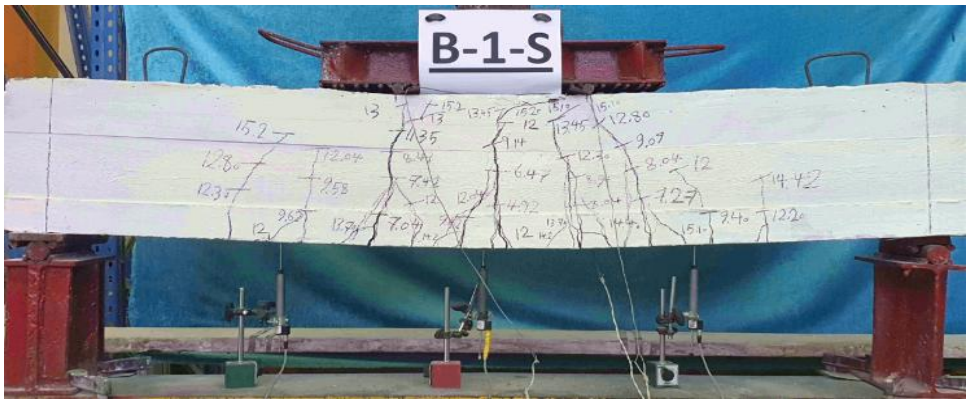

Figure 18. Conventional ductile flexural failure mode of beam B-1-S

Figures 17–19 depict the fracture pattern at failure of beams A–H-(6,7,9) constructed of normal strength concrete and HFRP-(B,D,F) carbon reinforcement bars. It's worth noting that all beams are put through their paces with increasing static loads until they fail. The first visible flexural cracks for beams A-6-H, A-7-H, and A-9-H made of carbon came at loads of 35 kN, 38.8 kN, and 36 kN, respectively. Beams A-6-H, A-7-H, and A-9-H all failed owing to flexure failure at ultimate loads of 105 kN, 122 kN, and 68 kN, respectively.

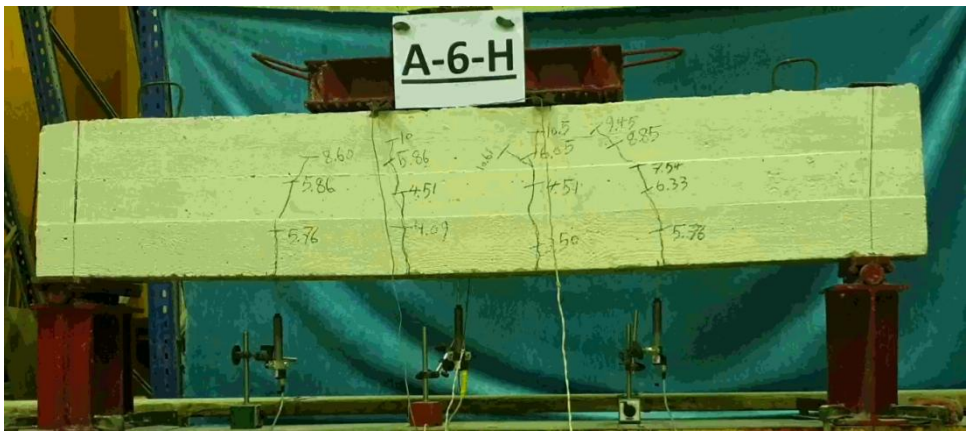

Figure 19. Ductile flexural failure mode of hybrid beam A-6-H.

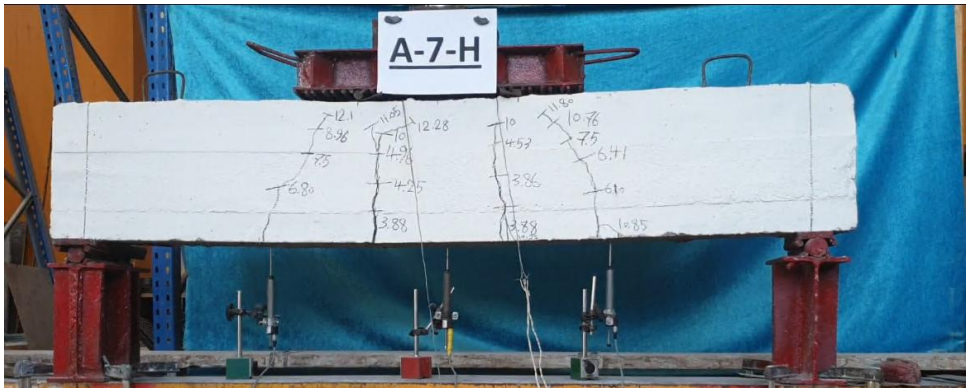

Figure 20. Ductile flexural failure mode of hybrid beam A-7-H.

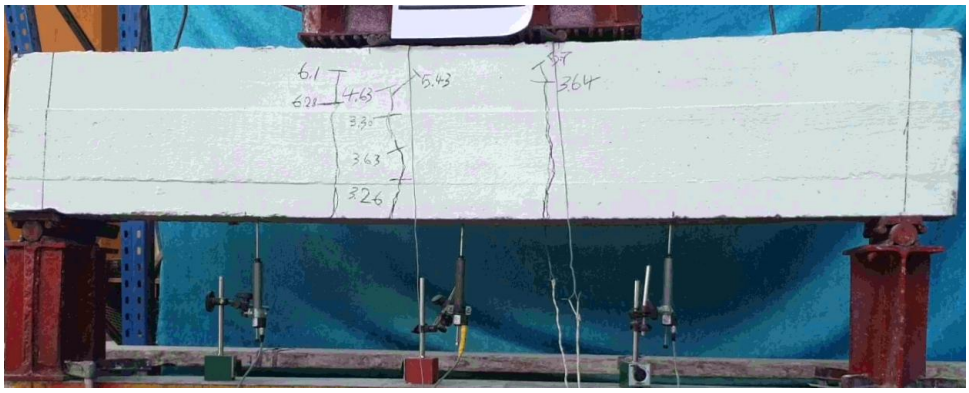

Figure 21. Ductile flexural failure mode of hybrid beam A-9-H.

Figure 22. For type (B,D, and F)"carbon type," the impact of hybridization in overcoming the rapid rupture.

Figures 21 and 22 depict the fracture pattern of beams B-H-(6,7) made of high-strength concrete HFRP-(B, D) carbon reinforcement at failure. It's worth noting that all beams are put through their paces with increasing static loads until they fail. The first visible flexural cracks appeared in carbon beams B-6-H and B-7-H with weights of 42 kN and 47.5 kN, respectively. Only flexure failure caused the failure of beams B-6-H and B-7-H with an ultimate load of 80 kN and 125 kN, respectively.

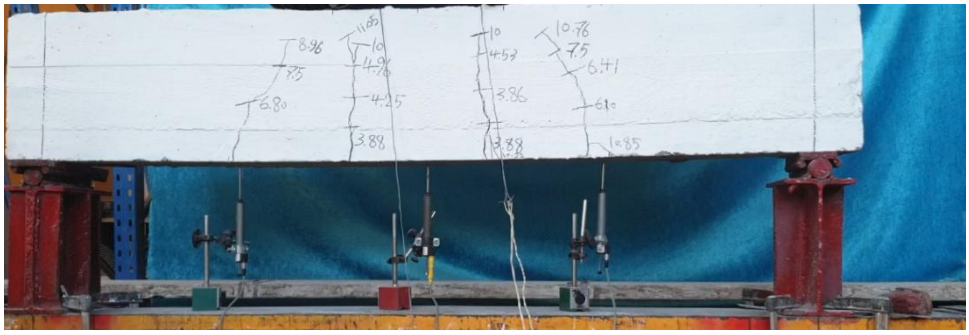

Figure 23. Ductile flexural failure mode of hybrid beam B-6-H.

Figure 24. Ductile flexural failure mode of hybrid beam B-7-H.

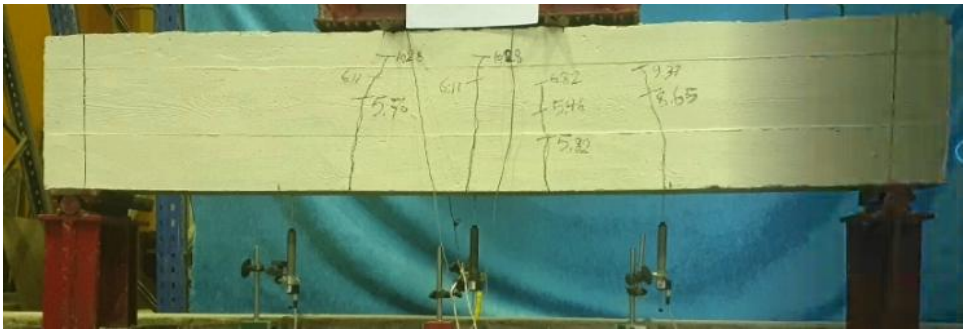

Table 4 first cracking and total experimental failure loads of beams tested

Beam Notation	**First Cracking Loads, P_{cr}(KN)**		**TOTAL EXPERIMENTAL FAILURE LOAD (KN)**	**Observed Failure Mode**
	Experimental	Theoretical		
A-1-S	40	32.80	134	Flexural-Tension Failure at mid-span
A-3-C	31.2	32.80	80	CFRP rupture
A-6-H	35	32.80	105	Flexural-Tension Failure at mid-span
A-7-H	38.8	32.80	122	Flexural-Tension Failure at mid-span
A-9-H	36	32.80	68	Flexural-Tension Failure at mid-span
B-1-S	49.2	47.4	152	GFRP rupture
B-3-C	50	47.4	90	Flexural-Tension Failure at mid-span

B-6-H	42	47.4	80	Flexural-Tension Failure at mid-span
B-7-H	47.5	47.4	125	Flexural-Tension Failure at mid-span

Table 5 Load responses of beams

Beam Notation	**Initial Stiffness (K)**	***Pu*** **KN**	**Deflection (mm) Under ultimate load, *Pu* (KN)**
A-1-S	20.67241	134.6	22
A-3-C	NA*	77.5	15.6
A-6-H	13.29412	110.5	13
A-7-H	20.40816	122.8	12.5
A-9-H	9.958333	64	8.5
B-1-S	24.10417	157.2	38
B-3-C	NA*	73	13.48
B-6-S	20	110.5	14.3
B-7-S	28	125.8	13.2

NA*Not applicable

Group (A)

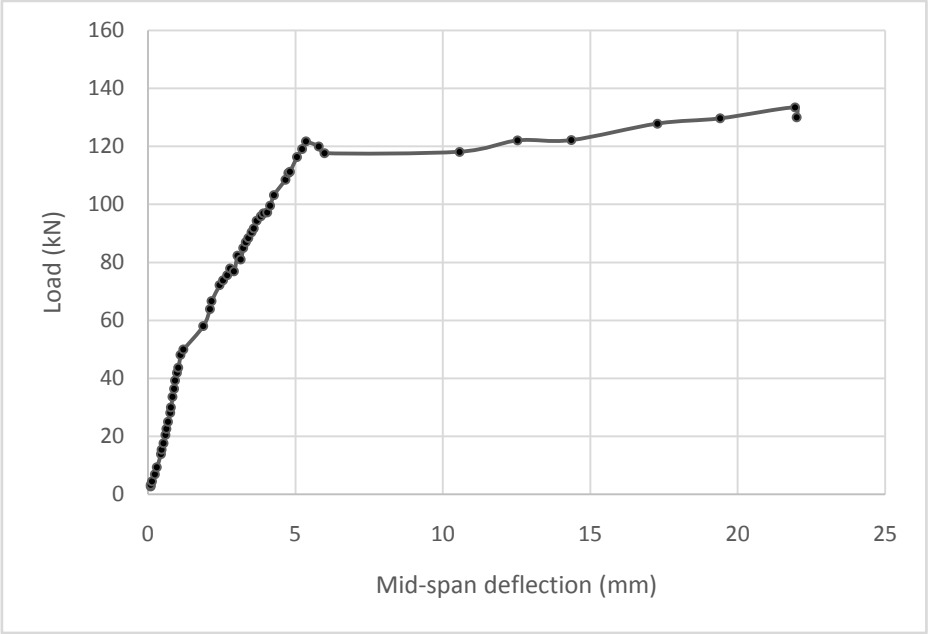

Figure 25. Load-deflection at mid-span for A-1-S tested beam.

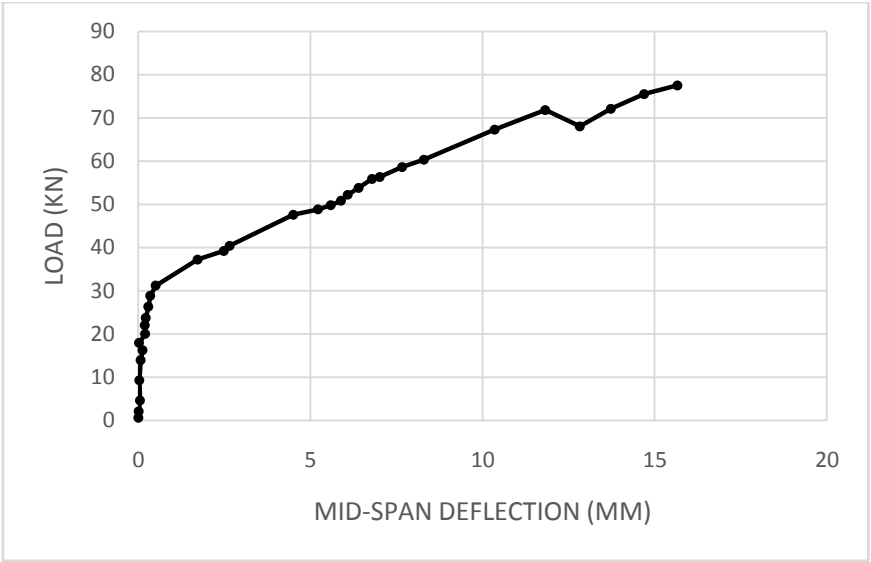

Figure 26. Load-deflection at mid-span for A-3-C tested beam.

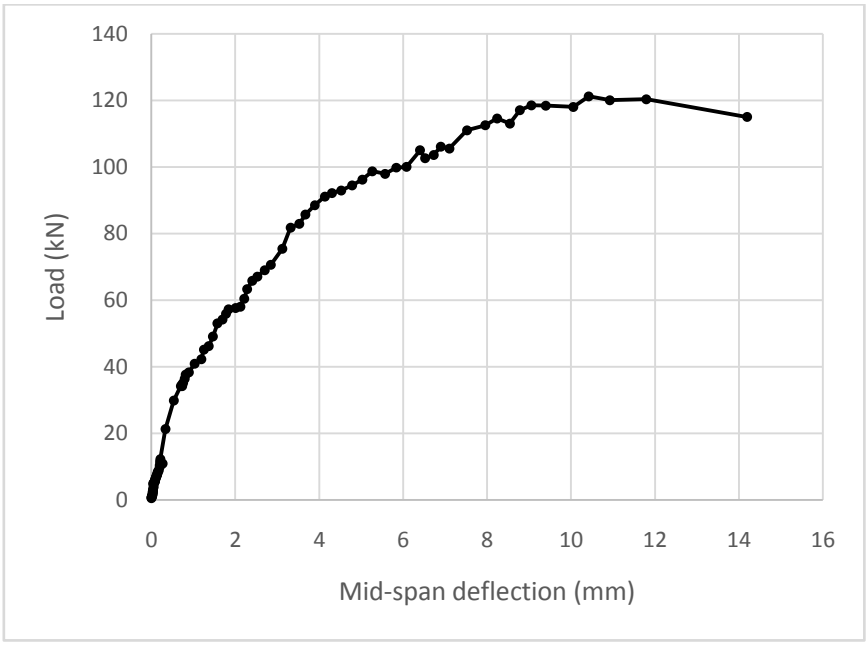

Figure 27. Load-deflection deflection at mid-span for A-6-H tested beam.

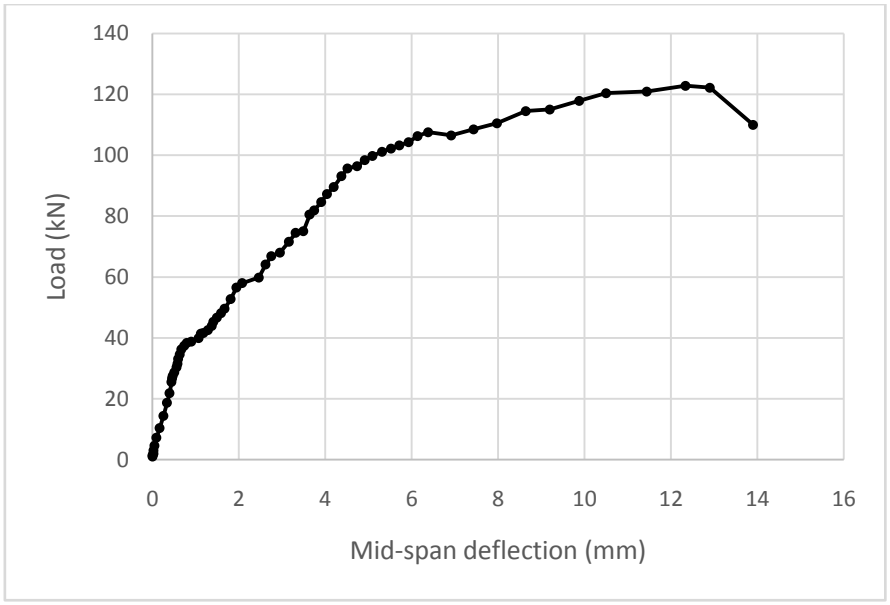

Figure 28. Load-deflection deflection at mid-span for A-7-H tested beam.

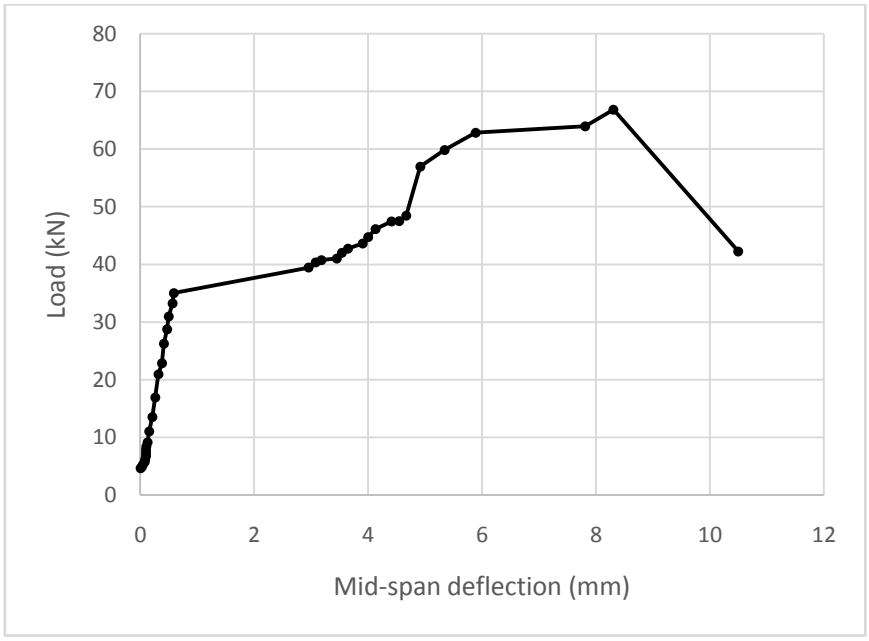

Figure 29. Load-deflection deflection at mid-span for A-9-H tested beam

Group (B)

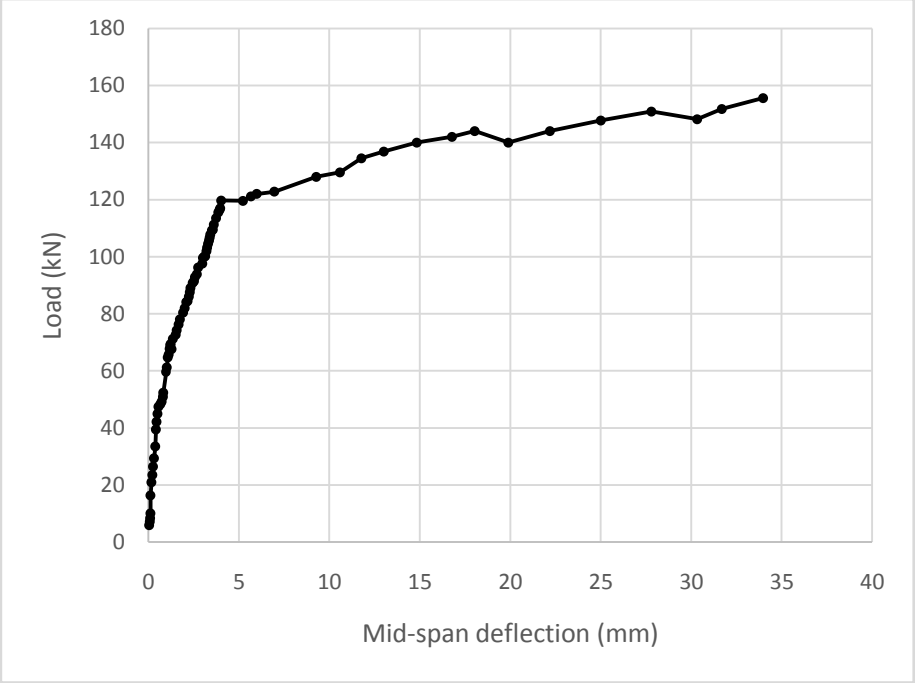

Figure 30. Load-deflection deflection at mid-span for B-1-S tested beam.

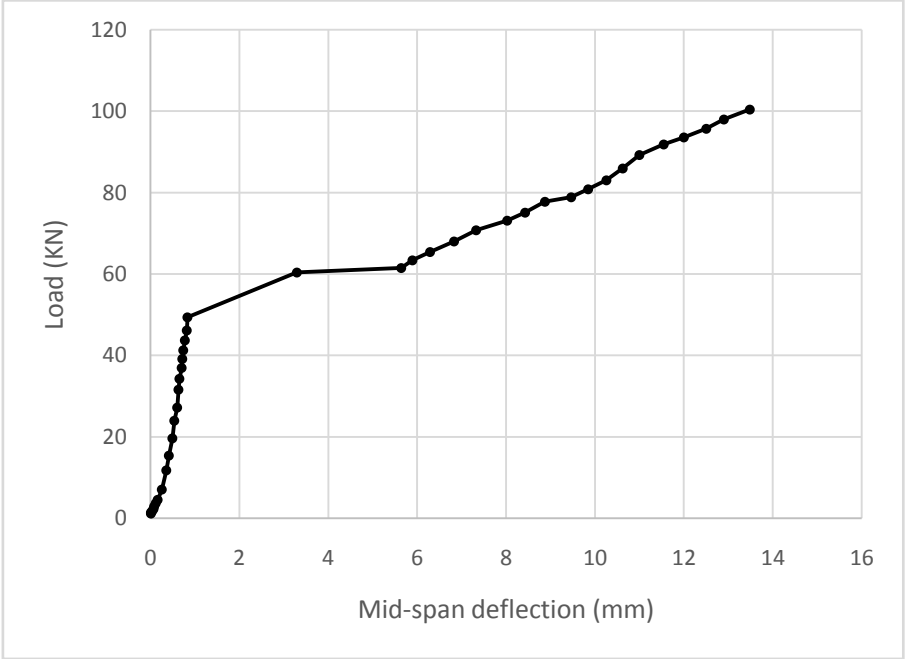

Figure 31. Load-deflection deflection at mid-span for B-3-C tested beam.

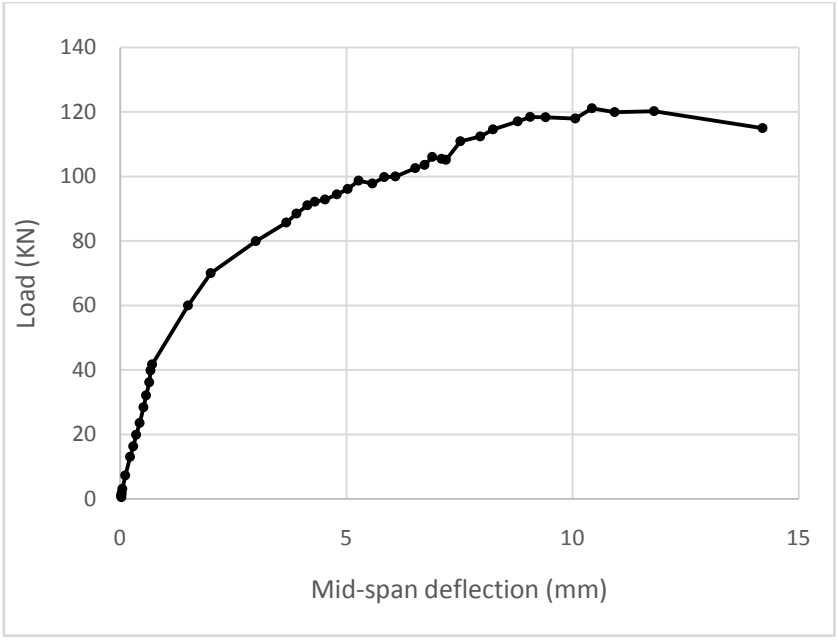

Figure 32. Load-deflection deflection at mid-span for B-6-H tested beam.

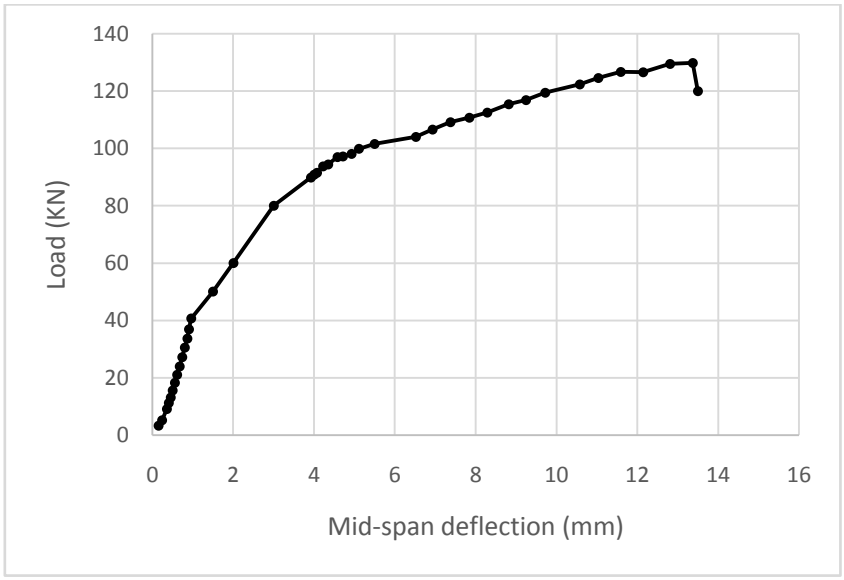

Figure 33. Load-deflection deflection at mid-span for B-7-H tested beam.

4. DISSCUSION

The flexural behavior of concrete beams reinforced with a newly invented locally made hybrid bar (HFRP) with a steel bar core was explored in this work. The employment of a CFRP crust with a steel core to make reinforcement bars looks to be a well-developed technology for usage in concrete structures. Initial uniaxial tensile testing showed that braiding FRP crust over a smooth steel rod produces a product of satisfactory quality. As a one-of-a-kind product, a semi-ductile hybrid FRP composite rebar was developed for usage in infrastructure construction projects. The hybrid FRP rebar has lower strength than conventional steel reinforcement, but it has better semi-ductility than any other CFRP reinforcing product on the market. To failure, the hybrid FRP bars showed bilinear elastic behavior with an elasticity modulus lower than steel.

5. CONCLUSIONS

A steel core added to a FRP bar boosted rigidity in the elastic and plastic regions, which CFRP bars lacked. To make the reinforcement work with different types of concrete, a designer might alter the thickness of the FRP crust, the diameter of the steel core, and the strength of the steel core.

The hybrid FRP rebar has greater semi-ductility than other types of FRP reinforcing materials and has a higher strength than standard steel reinforcement.

The semi-ductile mode of failure, for example, is produced by hybrid reinforcement yielding at lower stress rates, whereas CFRP beams have no reinforcement yielding, so the concrete breaks first by crushing. Hybrid reinforcements in concrete beams are believed to behave similarly to regular reinforcements when tested under pure tension.

A broad and deep fracture with concomitant significant deformations was an early warning indication of failure in beams reinforced with HFRP bars.

REFERENCES

[1] Code, E. (2005). The Egyptian Code of Practice on the Use of Fibre Reinforced Polymers in the Construction Fields, (ECP 208). HOUSING AND BUILDING NATIONAL RESEARCH CENTRE.

[2] Daniel, I. M., Ishai, O., Daniel, I. M., & Daniel, I. (2006). Engineering mechanics of composite materials (Vol. 1994). Oxford university press New York.

[3] Dholakiya, B. (2012). Unsaturated polyester resin for specialty applications. Polyester, 7, 167–202.

[4] El-Mihilmy, M. T., & Tedesco, J. W. (2001). Prediction of anchorage failure for reinforced concrete beams strengthened with fiber-reinforced polymer plates. Structural Journal, 98(3), 301–314.

[5] Elyazed, M. A., Eltahawy, R., EL-Nawawy, O. A., & Ragab, K. S. (2019). Flexural Behavior of Concrete Slabs Reinforced with Innovative Semi-Ductile Hybrid FRP Bars. International Journal of Scientific & Engineering Research, 10(6), 6–16.

[6] Frosch, R. J. (1999). Another look at cracking and crack control in reinforced concrete. Structural Journal, 96(3), 437–442.

[7] Gao, B., Leung, C. K. Y., & Kim, J.-K. (2007). Failure diagrams of FRP strengthened RC beams. Composite Structures, 77(4), 493–508.

[8] Gergely, P., & Lutz, L. A. (1968). Maximum crack width in reinforced concrete flexural members. Special Publication, 20, 87–117.

[9] Gross, S. P., Yost, J. R., Dinehart, D. W., Svensen, E., & Liu, N. (2003). Shear strength of normal and high strength concrete beams reinforced with GFRP bars. In High performance materials in bridges (pp. 426–437).